Multiple Self-Assembly Functional Structures Based on Versatile Binding Sites of β-Lactoglobulin

Netta Hendler, Bogdan Belgorodsky, Elad D. Mentovich, Shachar Richter, Ludmila Fadeev,* and Michael Gozin**

In recent years, research in the field of protein-based fibrils gained a great attention due to use of these materials as building blocks for construction of functional synthetic biofilms. Yet, efficient and general methodology for preparation of orderly-doped fibrils with desired properties, made of protein-dopant/ligand complexes, still remains a significant challenge. In this manuscript, it is demonstrated that the β-lactoglobulin (β-Lg) protein can form stable and well-defined complexes with linear retinoic acid, discotic protoporphyrine IX and spherical carboxyfullerene ligands (dopants). Upon heating these β-Lg complexes under acidic conditions, formation of orderly-doped fibrils, which partially preserved ligand-specific stoichiometries and modes of binding (of the parent protein-dopant complexes), is observed. These results present a new synthetic methodology, which complements other reported approaches for preparation of the protein-based doped fibrils, by surface functionalization and by post-assembly modulation techniques. A combination of ordered self-assembly nano-structures, with chemical versatility of the orderly-doped protein-based fibrils, represents a new method for construction of novel multifunctional materials in a bottom-up fashion. Preparation of composite β-Lg-complex fibrils by the co-assembly process, using β-Lg building blocks that already incorporate various organic ligands inside, is unprecedented.

1. Introduction

Certain proteins and polypeptides can readily self-assemble themselves into macromolecular fibrillar structures, through hydrogen-bonding interactions.[1] The resulting amyloid-like fibrils typically exhibit tubular structures, with sizes of few nanometers in diameter and lengths of a several thousand nanometers.[2] Amyloid-like fibrils are described as cross-β-sheet structures composed of intermolecular β-sheets, along the fibril axis, with the β-strands aligned perpendicularly to the fibril axis. These fibrils could be formed by proteins or peptides, with a wide variety of sizes and amino acid sequences. Formation of amyloid fibrils are frequently associated with several severe diseases, such as Parkinson's disease, Alzheimer's disease, diabetes, atherosclerosis and rheumatoid arthritis. In contrast, amyloid-like fibrils have important biological functions and are present in a variety of organisms, including Escherichia coli, silkworms, fungi and mammals.[3]

Amyloid-like fibrils were found to be stable in various environments, well beyond a typical range of chemical conditions tolerated by polypeptide-based structures,[4] which makes these fibrils very attractive platform for the development of novel bio-nanomaterials. For example, it was shown that by using self-assembly approach, free-standing films, based on amyloid fibrils, could be prepared. These films were found to be highly rigid and exhibited a well-ordered assembly. The Young's modulus measured for these films was of up to 5–7 GPa and, which is among the highest reported for protein-containing materials. The combination of accurate self-assembly, variability of amino acids sequence and possibility for further functionalization, the films based on amyloid-like fibrils represent an excellent example for building nanostructure in the bottom-up fashion. Recently, Ellis-Behnke *et al*. demonstrated that a network comprised of self-assembled polypeptide-based fibrils supports a sufficient axon regeneration to return functional vision to hamsters, in which an optic tract had been severed.[5] Others researchers explored the use of amyloid-like fibrils for tissue engineering.[6]

One of the new potential applications for biopolymer fibrils is their use in electronic applications. The utilization of self-assembled fibrils was successfully demonstrated in organic photovoltaic devices and organic light-emitting diodes (OLEDs).[7] It was found that inclusion of such fibrils into these devices influenced the electronic and transport properties of the light emitting materials. More specifically, the electroluminescent PPF-coated insulin fibrils showed an order of magnitude increase in external quantum efficiency of the blue light, relative to the neat polymer. The improved performance

B. Belgorodsky, L. Fadeev, Dr. M. Gozin
School of Chemistry
Raymond and Beverly Sackler Faculty of Exact Sciences
Tel Aviv University
Tel Aviv 69978, Israel
E-mail: givelberg@gmail.com;
cogozin@mgchem.tau.ac.il

N. Hendler, E. D. Mentovich, Dr. S. Richter
University Center for Nanoscience and Nanotechnology
Tel Aviv University
Tel Aviv 69978, Israel
E-mail: srichter@post.tau.ac.il

DOI: 10.1002/adfm.201102463

© 2012 WILEY-VCH Verlag GmbH & Co. KGaA, Weinheim

originates from enhanced electron injection and balanced charge-carrier mobility in the bio-organic device.

The performance and the efficiency of the organic electronic devices are intimately related to a molecular architecture of the self-assembled fibril-based building blocks. Three common approaches for construction of these building blocks are known in the field. The first is "*co-assembly*" bottom-up approach, which utilizes modification of polypeptide monomers, capable of the self-assembly, with electro-optically functional moieties. The second is "*post-assembly*" top-down approach, which utilizes surface-modification (in a covalent or non-covalent manner) of already-assembled polypeptide fibrils with the functional moieties. The third is an additional top-down approach, which makes use of polypeptide fibrils as tubular or linear template materials, for construction of electro-optically functional nano-materials.

Following the nanomaterial's formation, fibril template could be removed or kept, as an insulation moiety or a platform, for the further modification. Among presented approaches, the top-down techniques are the most frequently used for the fabrication of various electronic and optical devices.

It should be mentioned that the above-described bottom-up approach is limited by a variety of materials suitable for functionalization. Many of these materials are hydrophobic and their poor solubility in aqueous solutions could interfere with fibrils formation process, as well as with their subsequent dispersion. Another significant challenge in modified fibrils "co-assembly" is possible interference of functionalizing moieties with fibril assembly process itself, resulting in formation of amorphous aggregates.

In general, the "post-assembly" non-covalent top-down functionalization approach is chemically more mild and compatible with biomaterials. It is considered as advantageous over alternatives and therefore is more popular. Frequently, it is very difficult to rationally design a compound to be a specific ligand (modifying moiety) for a certain molecular host or surface, *even* if a high-fidelity structure of this host or surface are known. A non-covalent ligand binding is typically reversible, presenting a problem in homogeneity and stability of the resulted macromolecular assemblies. Functionalization chemistry that could be well-tolerated by a monomer, but not by the already-assembled fibril, may lead to a collapse of the fibril structure.

Yet, the main unresolved issue of the "*post-assembly*" approach remains to be a lack of capability to pinpoint the exact locations of modifying moieties, as well as very limited ability to predict assembly into desired macromolecular structures. Although the latter problem could be easier solved by the "*co-assembly*" techniques, it is still presents one of the most formidable challenges for materials engineering and rational design.

A plausible solution to this challenge may also come, for our opinion, from finding a proper "vehicle", which would carry the modifying moieties and would allow straightforward formation of non-covalently-bound well-organized macro-molecular assemblies with predictable architectures. To the best of our knowledge, formation an ordered macro-structure, composed of monomeric units that contain complex of a protein and organic ligands, is unprecedented and represents a new paradigm for next-generation "co-assembly" methodology. For these purposes, proteins that have several different well-defined binding sites, in addition to a capability (functional motifs, such as β-strands) to form macromolecular assemblies, could be used as suitable building blocks, thus reducing the challenge of finding and evaluating protein candidates and corresponding ligands. In this work, we explored a use of bovine β-Lactoglobulin (β-Lg) complexes, as building blocks for construction of functional fibrils.

β-Lg is a major whey protein, capable of binding a wide range of hydrophobic and amphiphilic ligands, including retinoids, fatty acids, aromatic molecules and porphyrins.[8] β-Lg belongs to family of proteins called lipocalins. Lipocalins are a large and diverse group of small, mostly extracellular proteins that are found in animals, plants, and bacteria.[9] The members of the lipocalin family fulfill a variety of different functions, many of which are associated with transport of various hydrophobic ligands, including retinoids, animal camouflage pigments, olfaction-related molecules, and pheromones.[9,10]

The three-dimensional structures of the lipocalins are typically comprise of anti-parallel eight-stranded β-barrels arranged to form a hydrophobic calyx-shaped cavity into which a variety of hydrophobic ligands can be bound, allowing these proteins to function as transport proteins for various sparingly water-soluble molecules.[9a,10]

At least two different binding sites have been proposed in the β-Lg dimer (a typical form of this protein). The location of the internal binding site inside–the β-barrel (calyx) is commonly accepted. This site can bind ligands such as retinol and piperine.[8b,11] In contrast, the exact locations of external sites of β-Lg dimer are less explored. Recently the first crystallographic evidence for vitamin D3, bound outside the calyx, was reported.[12]It was also suggested that fatty acids and other ligands could be bound outside the calyx, between a groove of the β-barrel and the α-helix.[8c,13] Moreover, it was previously shown that the β-sheets-rich β-Lg protein could be used for creation of fibrils (**Scheme 1**).[14] Taking in account these reports and assuming that various ligands could be bound to the specific binding sites of β-Lg dimer, without potentially interfering to a formation of fibrous macrostructure, the selected complexes of this protein were selected as target building blocks in our research.

Therefore, in the present study, we used complexes of β-Lg dimer with variously-shaped natural and synthetic ligands, for construction of fibrous materials exhibiting predictable fibrilar arrangement with homogenic incorporation of functional ligands, based on position of the bound ligands in the β-Lg dimer. First part of our work was focused on mapping the external binding sites of β-Lg and determination of plausible positions at which various ligands are bound. These ligands included all-trans-retinoic acid (RA), protoporphyrine IX (PP), and *eee*-isomer of trismalonic acid [C_{60}]-fullerene (carboxyfullerene, CF). The second part of this study was dedicated to preparation, characterization and functional evaluation of fibrils, formed by β-Lg complexes.

2. Results and Discussion

2.1. Formation and Characterization of the β-Lg Protein Complexes

2.1.1. Formation and Characterization of the β-Lg-RA Complex

Our study was commenced with a series of experiments in which we attempted to map various β-Lg's binding sites

© 2012 WILEY-VCH Verlag GmbH & Co. KGaA, Weinheim

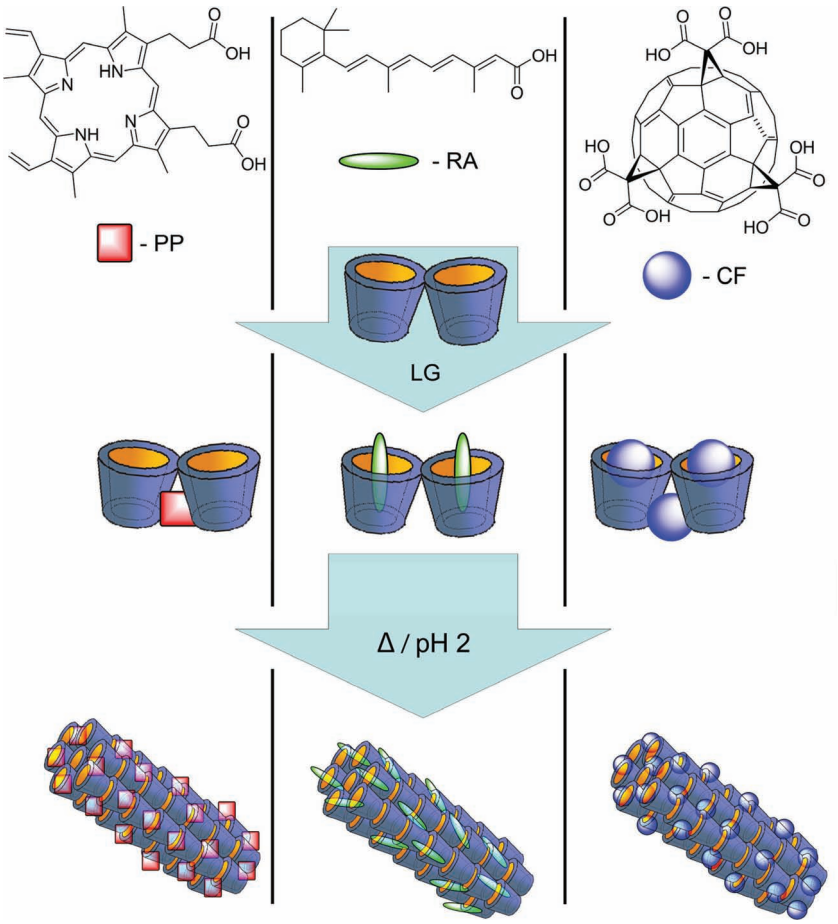

Scheme 1. Schematic representation of the ligand-doped "co-assembly" of fibrils comprised of β-Lg complexes.

and characterizing produced protein complexes by dynamic light scattering (DLS), size-exclusion chromatography (SEC) and UV-vis spectroscopy. RA was selected as a representative amphyphilic linear-type of ligand for binding to calyx and similar in shape binding sites.

The starting materials for this set of experiments were characterized DLS was measured for a β-Lg dimer solution in the phosphate buffer (50 mM, pH 7.2); the protein exhibited a hydrodynamic radius (R_h) of 2.4 nm (**Figure 1**a), in agreement with other investigators' results and X-ray crystallography data reported for this protein.[15] This R_h value of the β-Lg dimer corresponded to an SEC retention time (RT) of 15.9 min on the TOSOH SuperSW2000 column (Figure 1b). The UV-vis spectrum of the dimer is shown in Figure 1c.

Upon dissolving RA in a phosphate buffer solution (50 mM, pH 7.2), we found that this compound formed aggregates with a prevalent R_h of 600 nm (Figure 1d). To the best of our knowledge, no reports are available regarding the size of RA aggregates in aqueous solution. A dimethyl sulfoxide (DMSO) solution of non-aggregated RA had a characteristic peak at λ_{max} = 354 nm (Figure 1e), whereas the UV-vis spectrum of RA aggregates in buffered solution exhibited a peak at λ_{max} = 375 nm (Figure 1f).

The β-Lg-RA complex was prepared by incubating β-Lg dimer solution (0.075 mM) with RA ligand (final concentration 0.75 mM) in phosphate buffer (50 mM, pH 7.2). After 12 hours of incubation, the complexation products were analyzed by DLS (Figure 1g) and then separated by gel filtration chromatography (G-25 support) from non-complexed and unstable RA aggregates (Figure 1h). Two distinct populations of stable compounds were observed by SEC. The main product eluted with an RT of 15.8 min (closely matching the RT of the β-Lg dimer) and had a UV-vis spectrum (Figure 1i) with features of both β-Lg and RA chromophores (λ_{max} = 280 and 355 nm, respectively), clearly indicating that in this complex, the RA ligand is located in a non-aqueous (DMSO-like) environment, most probably inside the β-Lg's calyx.[15a]

The β-Lg-RA complex that eluted at RT of 15.8 min was isolated by SEC and further analyzed for protein and ligand content. The quantitation of β-Lg protein was performed by Bio-Rad protein assay (BPA), whereas RA content was measured by UV-vis spectroscopy at λ_{max} = 355 nm after selective extraction of this ligand with butanol-hexanes mixture.[16] These analyses showed a β-Lg monomer-to-ligand ratio of 2:2, which is in agreement with previously reported results for the β-Lg-RA complex.[15a,17]

The SEC peak that eluted at an RT of 10.3 min corresponded to a population of products observed by DLS with R_h values in a range of 20-300 nm. The UV-vis spectrum (λ_{max} = 377 nm) of these compounds was assigned to RA aggregates (Figure 1j). However, the size of these aggregates was significantly smaller than RA aggregates in the starting aqueous solution of RA. After separation by SEC, the aggregates were analyzed using the BPA. The assay clearly showed the presence of a small amount of protein (below 3% of content) in these aggregates.

2.1.2. Formation and Characterization of the β-Lg-PP Complex

In the second series of experiments, β-Lg dimer (0.075 mM) was incubated with PP (0.75 mM), under the same conditions that were described for complexation of RA. The PP compound was selected for these experiments as a representative discotic type of ligand. Upon dissolving PP in a phosphate buffer solution (50 mM, pH 7.2), we found that this ligand formed a population of PP aggregates with a narrow size range, with an average R_h value of 600 nm (**Figure 2**a). A UV-vis spectrum of PP in DMSO showed characteristic low intensity peaks at λ_{max} = 628, 574, 540, 505 nm and a high intensity peak at 406 nm (Figure 2b). In contrast, PP aggregated in a phosphate buffer solution and the UV-vis spectrum of these aggregates exhibited a broad peak at λ_{max} = 374 nm (Figure 2c). Our DLS and UV-vis spectroscopy results are in very good agreement with findings reported for aqueous solutions of PP by Scolaro et al.[18]

© 2012 WILEY-VCH Verlag GmbH & Co. KGaA, Weinheim

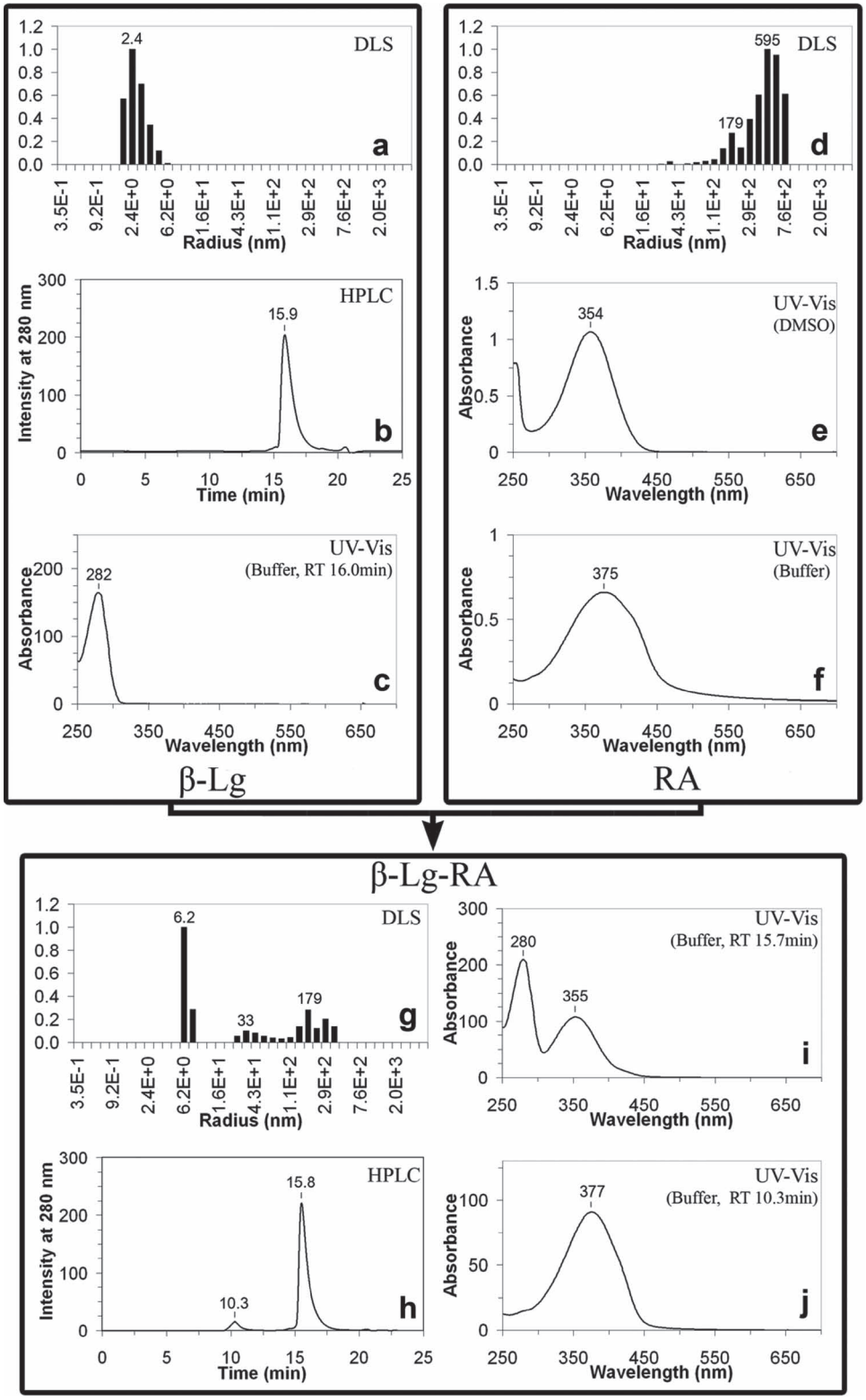

Figure 1. Characterization of β-Lg protein, RA ligand and β-Lg-RA complex. (a) DLS analysis of a 50 μM solution of β-Lg dimer in sodium phosphate buffer; (b) SEC of the β-Lg dimer. (c) UV-vis spectrum of β-Lg dimer eluted from SEC with RT of 15.9 min; (d) DLS measurements for RA aggregates in sodium phosphate buffer; (e) UV-vis spectrum of RA in DMSO. (f) UV-vis spectrum of aggregated RA in phosphate buffer; (g) DLS analysis of β-Lg incubated with RA (protein-to-ligand ratio of 1:10); (h) SEC analysis of products of β-Lg incubation with RA; a well-defined protein complex is eluted at RT of 15.8 min and stable RA aggregates eluted at RT of 10.3 min; (i) UV-vis spectrum of a well-defined β-Lg-RA complex eluted at RT of 15.8 min; (j) UV-vis spectrum of stable RA aggregates eluted at RT of 10.3 min.

© 2012 WILEY-VCH Verlag GmbH & Co. KGaA, Weinheim

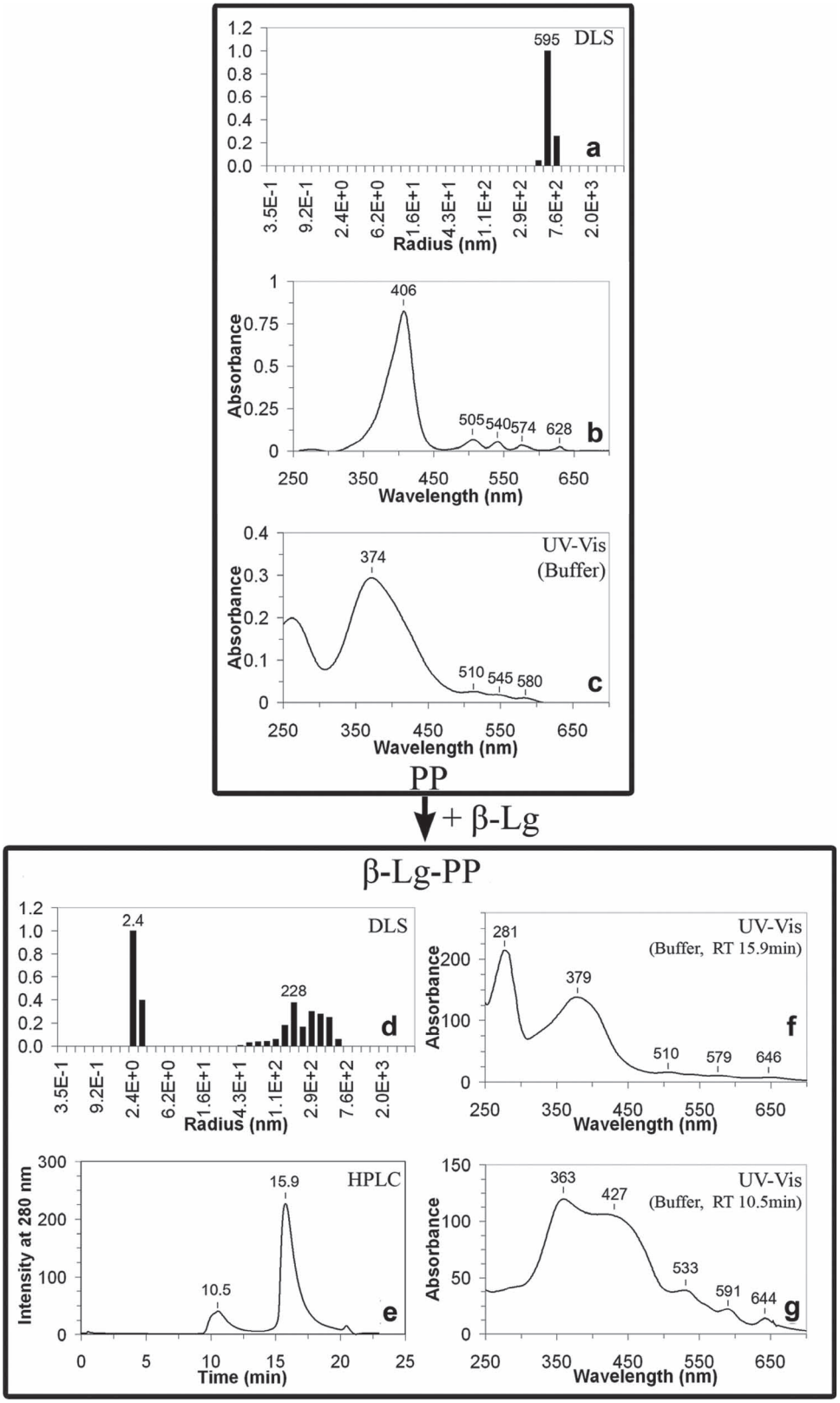

Figure 2. Characterization of PP ligand and β-Lg-PP complex. (a) DLS analysis of PP aggregates in phosphate buffer; (b) UV-vis spectrum of PP in DMSO; (c) UV-vis spectrum of aggregated PP in phosphate buffer; (d) DLS analysis of β-Lg incubated with PP (protein-to-ligand ratio of 1:10); (e) SEC analysis of products of β-Lg incubation with PP; a well-defined protein complex is eluted at RT of 15.9 min and stable PP aggregates eluted at RT of 10.5 min; (f) UV-vis spectrum of a well-defined β-Lg-PP complex eluted at RT of 15.8 min; (g) UV-vis spectrum of stable PP aggregates eluted at RT of 10.5 min.

© 2012 WILEY-VCH Verlag GmbH & Co. KGaA, Weinheim

Although PP ligand is not known to form complexes with lipocalins in biological systems, complex formation between PP and β-Lg at low μM concentrations was reported by several investigators.[19] At native concentrations (90–200 of μM) of β-Lg, we found that complexation with PP produced two populations of species with distinctive sizes. The DLS analysis of the complexation products (after G-25 column gel filtration) showed that the first population of species exhibited a size corresponding to β-Lg dimer, while the second population had a significantly broader range of sizes with an average R_h value of 300 nm (Figure 2d).

In addition, the SEC chromatogram of β-Lg and PP incubation products showed two peaks with RTs of 15.9 and 10.5 min (Figure 2e). The latter chromatographic peak had UV-vis spectrum with features corresponding to PP aggregates (Figure 2g), closely matching spectrum reported by Inamura for PP ligand dissolved in poly(n-vinyl-pyrrolidone) aqueous solution.[20] According to these investigators, the poly(n-vinyl-pyrrolidone) polymer broke down PP aggregates, by creating hydrophobic interactions with PP molecules. In our case, incubation of PP aggregates with β-Lg protein also reduced these aggregates size, as it did for aggregates of RA. BPA assay showed the presence of a small amount of protein (below 5% of content) which is serving as dissolving and stabilizing agent for these aggregates.

The UV-vis spectrum of the β-Lg-PP complex, eluted at RT of 15.9 min (λ_{max} = 379 nm, Figure 2f), clearly indicated that the PP ligand is not located in a hydrophobic environment and therefore could not be bound inside β-Lg's calyx. The protein content in the β-Lg-PP complex was determined by BPA, whereas the ligand content was determined by a procedure which included SDS-based protein denaturation, followed by solution acidification (adjustment to 0.8 M HCl concentration) and UV-vis spectroscopy quantitation of a protonated PP.[21] Unexpectedly, and in contrast to previous reports, we found that protein monomer-to-ligand ratio in the β-Lg-PP complex was 2:1, indicating that only a single PP ligand was bound by the β-Lg dimer. Based on these observations, we believe that PP ligand is bound in a cleft created by the two monomeric β-Lg units.

2.1.3. Formation and Characterization of the β-Lg-CF Complex

For the present investigation, CF was chosen as a representative spherical type of ligand. In our previous work, we described complex formation between CF ligands and β-Lg dimer (reference 19 and Supporting Information section). There, we reported that large CF clusters (formed in aqueous solutions) completely disintegrate upon addition of β-Lg dimer, producing a well defined β-Lg-CF complex with a protein monomer-to-ligand ratio of 2:5.

2.2. Docking Studies

To better understand our experimental results and gain structural insight into the ligand-β-Lg dimer interactions, we carried out a series of docking studies, in which PatchDock algorithm was used for mapping of the most probable binding sites of RA, PP and CF ligands onto the β-Lg dimer.[22] The docking calculations were performed without using any *a priori* data that might indicate the ligand binding sites. The coordinates of the X-ray structures of the bovine β-Lg dimer were obtained from the Protein Data Bank (PDB entry 1BSY), from which crystallographic water molecules were removed.[23] In this structure, the EF loop is opened (Tanford transition), allowing ligands entrance to the calyx binding site.[23,24] The coordinates of the RA and PP ligands were obtained from β-Lg complexed with RA and ferrochelatase with protoporphyrin IX (PDB ID 1GX9 and 2HRE, respectively),[15a,25] whereas coordinates of the CF ligand were obtained by geometry optimization and DFT energy minimization calculations (Gaussian 03 software).

2.2.1. Docking Studies of β-Lg-RA Complexes

The first series of docking calculations was performed with the RA ligand. The best docking results for this essentially linear ligand were obtained when RA was accommodated inside the cavity formed by β-Lg's calyxes (**Figure 3**a). Two calyxes are available per β-Lg dimer and both were found to be occupied by two sequentially added RA ligands, in agreement with the experimentally determined β-Lg monomer-to-ligand ratio of 2:2. In contrast, the outer surface of the protein provided no specific binding environment for RA. The docking calculations suggested that binding of the RA molecule may occur in two possible fashions: the RA ring may be positioned at the open entrance of the cavity or may be buried deep inside the calyx.[11] However, only the latter arrangement is in agreement with the X-ray crystallography results for the β-Lg-RA complex.[15a] In this arrangement, our calculations showed that within van der Waals contact distance (less than 4.0 Å),[11] the conjugated hydrocarbon chain and ring of the RA ligand are surrounded by 11 hydrophobic residues (Pro38, Leu39, Val41, Leu46, Leu54, Ile56, Leu58, Ile71, Val92, Leu103, and Met107) that cover the inner surface of the calyx's cavity (Figure 3b). Additionally, the aromatic residue Phe105 was oriented to allow a π–π interaction with the double bond of the ring of the RA molecule. Hydrogen bonds could be formed between the carboxylic moiety of the RA ligand and two positively charged residues (Lys60 and Lys69), both located at the entrance of the calyx. Overall, our docking studies clearly indicate that RA ligand is bound to β-Lg predominantly by hydrophobic interactions, adequately explaining results obtained by UV-vis spectroscopy for the β-Lg-RA complex.

2.2.2. Docking Studies of the β-Lg-PP Complex

The best docking results for the planar PP ligand were obtained when PP was accommodated in a deep cleft located at the interface between two monomeric units of β-Lg (Figure 3c). The entry to this cleft is defined by two α-helixes, each belonging to a one monomer. The PP ligand is too large to enter the calyx cavity and too hydrophobic to be bound on the outer surface of the protein. The cavity size of the β-Lg dimer cleft allows convenient binding of a single PP ligand per dimer (Figure 3d), matching the experimentally found monomer-to-ligand ratio of 2:1. For this mode of binding, our calculations showed that within van der Waals contact, the discotic and amphiphilic PP

© 2012 WILEY-VCH Verlag GmbH & Co. KGaA, Weinheim

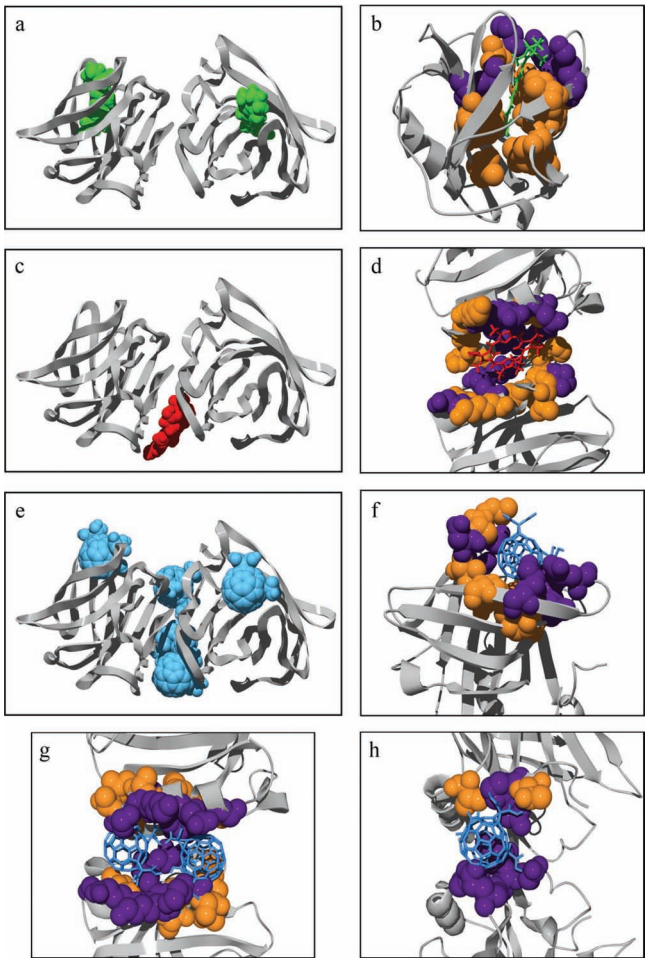

Figure 3. (a) The overall view of the high-score docking result for β-Lg-RA complex with monomer-to-ligand ratio of 2:2, in which the β-Lg is presented as a ribbon model (gray) and the RA ligands as space-filling models (green); (b) Hydrophobic (orange) and charged (purple) residues forming the calyx binding site of β-Lg are presented as space-filling models with the RA ligand (green); (c) The overall view of the high-score docking result for the β-Lg-PP complex with monomer-to-ligand ratio of 2:1, in which the β-Lg is presented as a ribbon (gray) and the PP ligands as space-filling models (red); (d) Hydrophobic (orange) and charged (purple) residues forming cleft binding site of β-Lg are presented as space-filling models with PP ligand (red); (e) The overall view of the high-score docking result for β-Lg-PP complex with monomer-to-ligand ratio of 2:5, in which the β-Lg is presented as ribbon model (gray) and the PP ligands as space-filling model (blue); (f) Hydrophobic (orange) and charged (purple) residues forming calyx binding site of β-Lg are presented as space-filling models with CF ligand (blue); (g) Hydrophobic (orange) and charged (purple) residues forming cleft binding site of β-Lg are presented as space-filling models bound to two CF ligands (blue); (h) Hydrophobic (orange) and charged (purple) residues form additional CF binding site (near the cleft) presented as space-filling models with CF ligand (blue).

ligand is surrounded by hydrophobic and hydrophilic residues of β-Lg dimer. We found that each monomer of β-Lg interacted with PP through the same set of amino acids. Per monomer, five hydrophobic (Leu133, Leu140, Leu143, Pro144 and Met145) and seven polar (Asp130, Glu131, Glu134, Asp137, Lys138, His146 and Arg148) residues created an appropriate surface for PP ligand binding. Specifically, positively charged His146 and Arg148 residues were positioned in a proximity to the carboxylic acid functional groups of PP, while negatively charged Asp137 was located near the center of a porphyrine moiety.

2.2.3. Docking Studies of β-Lg-CF Complexes

The third series of docking calculations was performed with the CF ligand, expanding our previously reported work with this ligand, in which CF was bound to a β-Lg structure with a closed calyx (in the present calculations the calyx is opened). Based on the experimentally observed β-Lg monomer-to-ligand ratio of 2:5,[26] we performed our docking calculation in a stepwise manner, sequentially adding a total of five CF ligands to a β-Lg dimer (Figure 3e). The docking results positioned the first and the second CF ligands at the cleft site, while the third and the fourth CFs showed preferential binding at the entrance of the β-Lg calyxes. Finally, the fifth CF ligand bound between two β-Lg monomers, but outside the cleft. The cleft surface, suitable for symmetric binding of two CF ligands, was formed by seven hydrophobic (Leu133, Phe136, Ala139, Leu140, Ala142, Leu143 and Met145) and three positively charged (Lys138, Lys141 and Arg148) residues per each β-Lg monomer (Figure 3g). As expected, CF was too large to enter the inner cavity of the calyx. However, the shape of this ligand and topology of carboxylic functional groups promoted a very good ligand interaction with positively charged residues (Lys60 and Lys69) positioned at the calyx's entrance (Figure 3f). CF bound near the calyx entrance was positioned near eight hydrophobic residues (Leu39, Val41, Leu58, Ile71, Ile84, Ala86, Leu87 and Met107. The fifth CF ligand was bound near the cleft site (Figure 3h); there were an insufficient number of hydrophobic and positively charged residues to provide strong interaction with the ligand at this site. We found that only two hydrophobic (Val128 and Thr154) and one positively charged (His146) residues were in a close proximity to the fifth CF. The other six residues forming this site (Ser27, Asp28, Glu114, Pro144, Asn152 and Pro153) do not seem to contribute to the ligand binding. Overall, our docking studies clearly indicate that hydrophobic CF ligands are bound to β-Lg dimer at three possible sites with degree of affinity corresponding to a number of hydrophobic residues at the site.

2.3. Fibrils Formation Based on β-Lg Complexes

Following the preparation of β-Lg complexes with differently-shaped ligands and mapping these ligands locations, we proceeded with the construction of the corresponding fibrils. The fibril co-assembly formation was achieved by heating sodium phosphate buffer solutions of β-Lg complexes to 80 °C for 24-48 h. (Scheme 1). Then, the resulted fibrils were examined by HRSEM, florescence microscopy (in cases of PP and RA ligands) and HRTEM (in case of CF ligand).

β-Lg was selected as a building block for fibrils construction due to this protein features, related to latter protein's proposed biological function. A hint regarding the function of β-Lg was obtained by comparison of its amino acid sequence with serum retinol-binding protein. The comparison between these

© 2012 WILEY-VCH Verlag GmbH & Co. KGaA, Weinheim

proteins revealed a great deal of similarity and indeed, β-Lgs from several species have been found to bind retinol. The role of serum retinol-binding protein is to transport vitamin A and D3 in a circulation, suggesting that the homologous β-Lg may function in a similar fashion, by binding and transporting retinoids, as was shown by Mao, Chen and coworkers.[12] More specifically, β-Lg may facilitate the absorption of vitamin A from milk, thus protecting its ligands from degradation under strong acidic environment of a stomach.[27] Not surprisingly, it was reported that β-Lg has an enhanced structural stability and exhibits resistance to completely losing its secondary structure, even under strongly acidic conditions.[11,13]

Such partially β-Lg folded form has been characterized by several investigators as a molten globule state.[28] The concept of a thermodynamically stable state on the folding pathway has been useful in explaining the process of protein denaturation induced by various means such as pH adjustment and heat treatment.[29] β-Lg has been proposed to exist in a molten globule state by Roefs and de Cruif.[30] Das et al. results indicated that β-Lg refolding process upon cooling this protein solution from 70 to 25 °C proceeds *via* structures having characteristics of a molten globule state.

With respect to changes in the β-Lg's tertiary structure and retinoids-binding properties, as a function of pH, it was reported that β-Lg exhibited very similar characteristics at pH 2.0 and pH 7.0. It has been concluded that the existence of the central cavity of the β-Lg calyx is pH independent, allowing access of various hydrophobic ligands to this cavity at broad range of pHs.[29] From these data and our own observations of fibrils formation (from above described β-Lg complexes), we would like to propose that the "*co-assembly*" construction in case of this protein was mostly possible due to β-Lg-ligand complexes relative stability at fibril-formation conditions (80 °C and pH 2, Scheme 1).

We next examined the "*co-assembly*" formation process of fibrils, in terms of incorporated ligand quantities and compared the results to the "*post-assembly*" methodology, used for the preparation of the same type of materials. At the end of each process, prepared by each methodology doped fibrils (including doped fibrils prepared by a reference "*zussamen*" process, see Supporting Information) were separated from non-fibrilled materials and fibrillation by-products by dialysis (using membrane with 100 kDa cut off) and lyophilized. Amount of ligands, in each type of doped fibrils, was determined spectroscopically (UV-vis, *versus* appropriate reference standard) after hydrolysis/extraction procedure (see Supporting Information). Specifically, we found that in case of the CF and PP, the content of these ligands in corresponding doped fibrils, prepared by the "co-assembly" methodology were 19% and 3.7%, respectively; and corresponded to the amounts of these ligands in the β-Lg-CF and β-Lg-PP complexes. In contrast, the content of these ligands in doped fibrils, prepared by the "*post-assembly*" methodology was 37% and 33%, respectively, indicating completely different loading of the latter fibrils.

2.4. Fibrils Characterization

In order to explore the structural and optical properties of our fibrils, High-resolution Scanning and Transmission Electron Microscopy (HRSEM and HRTEM), fluorescence spectroscopy and microscopy measurements were performed. **Figure 4** shows obtained HRSEM images. It can be clearly seen that for all samples, the fibrils formed by β-Lg complexes and fibrils composed of non-complexed protein had practically the same structure and closely resembled previously reported images of non-covalently-assembled fibers.[31] More specifically, in the cases of β-Lg-CF and β-Lg-PP complexes, the obtained bundles of fibrils exhibited length of several tens of micrometers and had a typical diameter of ~ 1 μm. In contrast, the β-Lg-RA complex-based bundles had a similar length, but exhibited

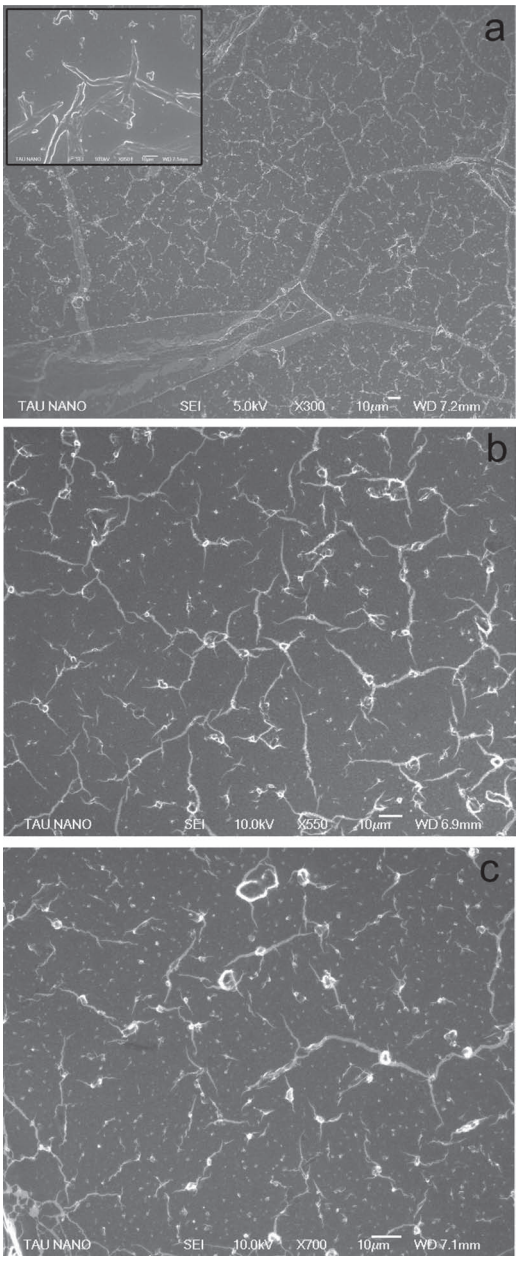

Figure 4. HRSEM characterization. Scale bar: 10 μm (a) HRSEM of β-Lg-RA fibrils; (b) HRSEM of β-Lg-PP fibrils; (c) HRSEM of β-Lg-CF fibrils.

© 2012 WILEY-VCH Verlag GmbH & Co. KGaA, Weinheim

a thicker diameter of several micrometers. Similar types of bundles were reported by Inganäs and coworkers in the case of post-assembly construction of insulin and thiophene-containing oligomers.[31] Our HRSEM measurements revealed that the "co-assembly" process does not alter the fibril formation, thus allowing us to construct various types of fibrils using this method.

In the case of β-Lg complexes containing fluorescent ligands, such as PP and RA, fluorescence spectroscopy and microscopy measurements were performed in order to evaluate the presence of these ligands in the corresponding fibrils. **Figures 5**b and 5c show the fluorescence spectra of dispersions of the β-Lg-PP and β-Lg-RA complexes, taken at pH 7 (before fibril formation) and pH 2 (fibril state). While negligible similar emission was found in the case of the pure β-Lg (Figure 5a) in both pHs' strong emission has been measured in the case of PP and RA complexes. Figure 5b shows the emission spectra of the RA complexes. It can be seen that fibril complex shows similar emission peak to that of the non-fibrilous one. However, in the case of the PP, a red-shift of the higher-energy peak has been observed in case of the fibril state, as observed previously.[32]

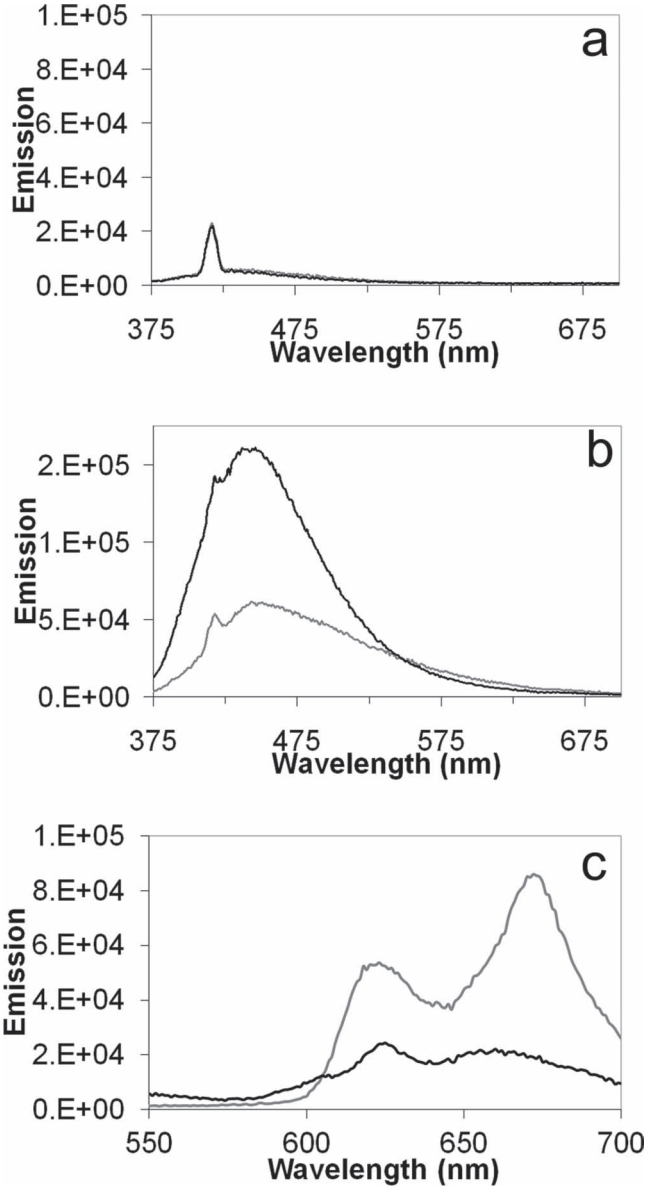

Figure 5. Fluorescence spectroscopy: (a) β-Lg in native form at pH 7 (black), β-Lg in fibril form at pH 2 (grey); (b) β-Lg-RA in native form at pH 7 (black), β-Lg-RA in fibril form at pH 2 (grey); (c) β-Lg-PP in native form at pH 7 (black), β-Lg-PP in fibril form at pH 2 (grey).

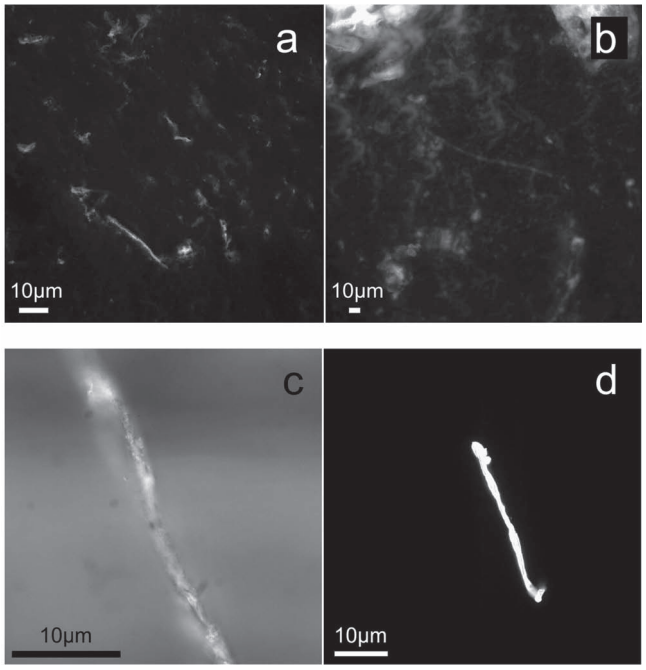

Figure 6. Fluorescence microscopy. (a) & (b) β-Lg-RA in fibril form at pH 2, (λ_{ex} = 360 nm); (c) β-Lg-PP in fibril form at pH 2, bright field; (d) β-Lg-PP in fibril form at pH 2 (λ_{ex} = 360 nm).

Typical fluorescence emission at 620, 670 nm (assigned for PP fluorophore) and 440 nm (assigned for RA fluorophore) obtained from the fibrils, clearly indicating the presence of the fluorescent ligands inside the fibrils' structures. In addition, these observations are supported by the corresponding fluorescence microscopy images, showing strong emission from the fibrils (**Figure 6**). In the fluorescence images, the diffused light emission that appears in the background stems from the emission of individual fibrils or small aggregates of fibrils. In addition, a small number of strongly emitting dot-shaped objects are present, which might be due to small clusters formed in the case of RA complexes structures.

While the TEM is used to verify that the CF ligands were incorporated inside the fibril, the fluorescent microscopy results clearly showed that we indeed created a fibrilous structure, as previously reported.

Figure 7 shows the HRTEM images obtained at different magnifications of the β-Lg-CF complex-based fibrils. One should note that for the other types of fibrils, HRTEM measurements are not very useful since in most cases the ligands are not exhibiting preferred crystallographic orientations. High magnification images taken at Scherzer defocus, demonstrate the crystallinity

© 2012 WILEY-VCH Verlag GmbH & Co. KGaA, Weinheim

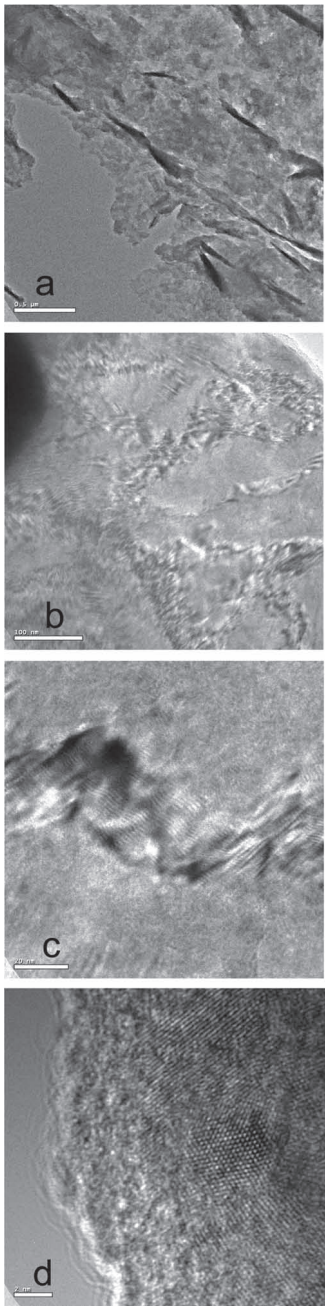

Figure 7. TEM of β-Lg-CF fibrils. Scale bars: (a) 0.5 μm; (b) 100 nm; (c) 20 nm; (d) 2 nm.

of the CF ligand in the β-Lg-CF complex-based fibrils, by the presence of lattice fringes. It is also observed that the latter fibril (with a typical diameter of above 2 nm) has CF ligands, ordered along the main axis of the fibril and positioned in a way that each ligand slightly overlaps the neighboring ligand.

3. Conclusions

In summary, in this work we prepared and structurally characterized a series of β-Lg protein complexes, with variously shaped ligands having different electronic and photo-physical properties. We have demonstrated that the resulted non-covalent complexes of β-Lg can function as building blocks for the construction of highly-doped fibrillar structures. These structures exhibited a minimal perturbation in their architecture, as compared to the fibrils formed by apo-β-Lg (non-complexed protein).

It was demonstrated that β-Lg could serve as a versatile host for a number of various ligands, allowing the generation of a series of different β-Lg-based fibrils, with specific material properties. β-Lg was selected for our study as a key component having intriguing properties. It is believed that in biological systems, the calyx motif of β-Lg can survive (for some time) harsh conditions of the digestive system, protecting its vitamin "payload".

Our new "co-assembly" process takes advantage of these special biochemical properties of the β-Lg, which become very handy for the construction of highly-doped fibrils, under low pH and elevated temperature conditions. We assume that under these conditions the protein transforms into its molten globule state. Subsequently, the unfolded non-calyx residues ("tentacles") participate in the fibrillar self-assembly process, while the calyx is still capable of retaining its ligand/dopant "payload".

The comparison of material obtained by our "co-assembly" method to the doped fibrils generated by the "post-assembly" methodology clearly indicates that our bottom-up process leads to new type of ordered materials. Specifically, a closer look at the ligand ratios in the doped fibrils of β-Lg, prepared by the co-assembly method, show that in our case these ratios are in a good correlation with ligand-to-protein ratios found by us in well-defined β-Lg-ligand complexes. Thus, we believe that our co-assembly methodology allows ordered ligands' incorporation into fibrils.

The future goals of this research will include the preparation of β-Lg complexes-based fibrils, carrying two or more different ligands/dopants that could be utilized for the construction of highly-resolved color-separated nano-taggants, diagnostic materials and optoelectronics components.

4. Experimental Section

Materials: The mixture of β-Lg A and B genetic variants, RA, and PP were obtained from Sigma-Aldrich and used as supplied. CF was synthesized according to previously reported methods.[33] All other reagents were of analytical grade. HPLC-grade water and organic solvents were used for all procedures and analyses.

Preparation of β-Lg Complexes with Various Ligands: Stock solutions of β-Lg dimer (100 μM) in sodium phosphate buffer (50 mM, pH 7.2), PP (100 mM) in acidic aqueous acetone (65% acetone in 0.8 M HCl), CF (100 mM), and RA (100 mM) in DMSO were used for preparation of β-Lg complexes and competitive binding studies. Typical complexation mixtures contained 75 μM β-Lg and 750 μM ligand in sodium phosphate buffer (50 mM, pH 7.2; with 0.8% of organic solvent). These mixtures were incubated at 37 °C for 2 h with stirring and then at 10 °C overnight. The complexation products were separated from non-complexed ligands on a Sephadex G-25 gel-permeation column (PD-10, Pharmacia Biotech) using sodium phosphate buffer (50 mM, pH 7.2) as an eluent.

Quantification of Protein and Ligand in β-Lg Complexes: The amount of β-Lg protein in samples was quantified by Bradford protein assay (BPA, BioRad). The amount of CF ligand in samples was determined spectrophotometrically (at λ_{max} = 485 nm, ε = 4,800 $M^{-1}cm^{-1}$).[26] The amount of PP ligand in samples was determined spectrophotometrically after acidification with concentrated HCl (to a total concentration

© 2012 WILEY-VCH Verlag GmbH & Co. KGaA, Weinheim

of 0.8 M HCl), by measurement of protonated PP (at λ_{max} = 406 nm, ε = 242,000 $M^{-1}cm^{-1}$).[21] The amount of RA ligand in samples was determined spectrophotometrically (at λ_{max} = 350 nm, ε = 45,000 $M^{-1}cm^{-1}$), directly or after quantitative extraction with a mixture of butanol and hexanes (1:1 v/v).[16,34]

Size-exclusion Chromatography: All size-exclusion chromatography (SEC) analyses were performed on an Agilent 1100 chromatograph equipped with diode-array detector. The analyses of β-Lg dimer, its complexes with RA, PP, and CF ligands and corresponding aggregates were performed on a 4.6 mm × 30 cm TSK-gel Super SW2000 column (Tosoh Bioscience) using a sodium phosphate buffer (150 mM sodium phosphate, pH 7.2 with addition of 150 mM of sodium chloride) as an isocratic eluent at 0.2 mL/min flow rate.

Dynamic Light Scattering: Particle size measurements were performed at 25 °C using ALV-NIBS/HPPS particle size analyzer (ALV-Laser Vertriebsgesellschaft). The particle size was calculated by the auto-correlation function of the ALV sizer software. Typically, analyzed solutions contained 50 μM concentrations of β-Lg dimer, PP, RA, or CF ligand in sodium phosphate buffer (50 mM, pH 7.2). Prior to dynamic light scattering (DLS) measurements, all mixtures of β-Lg complexes and corresponding aggregates were brought to the total protein concentration of 50 μM.

Docking Studies: The structure of β-Lg dimer used for docking calculations was obtained by alignment of the β-Lg apo-protein structure with opened EF loop (PDB ID 1BSY) onto the PDB ID 1BEB structure.[23,35] The coordinates of RA and PP were obtained from the crystallographic structures of β-Lg complexed with RA and ferrochelatase with protoporphyrin IX (PDB ID 1GX9 and 2HRE, respectively).[15a,25] Geometry structure optimization for the CF ligand was calculated by Gaussian 03 software using the DFT method with B3LYP force field. The docking calculations were performed by PatchDock algorithm without using any a priori data that might indicate the putative ligands binding sites.[22] The docking results were visualized with Swiss PDB Viewer (SIB) and Chimera (UCSF) software.[36]

Preparation of Fibrils Based on β-Lg-ligand Complexes, Using Co-assembly Methodology: To a solution of β-Lg dimer complex (2 mg/mL, 1 mL) in a sodium phosphate buffer (50 mM, pH 7.2) aqueous HCl (1.0M) was added dropwise to the final pH of 2.0 (approximately 10 mM final concentration). Than the resulted solution was filtered through cellulose filter (0.45 μm, Minisart, Sartorius) and then heated to 80 °C and kept at this temperature for 24-48 h in order to induce fibril formation.

High Resolution Scanning Electron Microscopy: All samples were prepared by drop casting of the fibril solution on a 10 × 10 mm piece of a highly doped silicon wafer (Silicon Quest). The surface was scanned by JSM-6700 Field Emission Scanning Electron Microscope operated at 5-10 kV.

Fluorescence Microscopy: The fibril samples were incubated overnight in room temperature, the emission spectra and time lapse data were taken with an Olympus upright microscope (BX51WI) fitted with an EMCCD camera (Andor Ixon-885) and a ×40 water immersion objective (Olympus, LUMPLFL NA 0.8).

This setup allows the visualization of fibril on top of non-transparent electrodes. Fluorescent excitation was provided *via* 120 W mercury lamp (EXFO x-cite 120PC) coupled to dichroic mirror with a filter to match the dye spectrum (Chroma T495LP). Camera control utilized Andor propriety SOLIS software.

High Resolution Transmission Electron Microscopy: All specimens were prepared by drop casting the fibril solution on top of an uncoated 2000 mesh copper grids (SPi) and examined by high-resolution transmission electron microscopy (HRTEM), operated at 200 kV (Philips F20). The structure evolution of the samples was recorded by an electron sensitive video camera (Gatan 622 SC) at 25 frames per second and examined frame by frame using Premiere software.

Supporting Information

Supporting Information is available from the Wiley Online Library or from the author.

Acknowledgements

The authors thank the Tel Aviv University and the Israeli Science Foundation for their generous financial support.

Received: October 12, 2011
Revised: January 9, 2012
Published online: May 23, 2012

[1] a) C. M. Dobson, T. P. Knowles, A. W. Fitzpatrick, S. Meehan, H. R. Mott, M. Vendruscolo, M. E. Welland, *Science* **2007**, *318*, 1900–1903; b) T. P. J. Knowles, M. J. Buehler, *Nat. Nanotechnol.* **2011**, *6*, 469–479; c) A. M. Donald, M. R. H. Krebs, G. L. Devlin, *Biophys. J.* **2009**, *96*, 5013–5019; d) K. Channon, C. E. MacPhee, *Soft Matter* **2008**, *4*, 647–652.

[2] a) I. W. Hamley, *Angew. Chem. Int. Ed.* **2007**, *46*, 8128–8147; b) T. P. J. Knowles, T. W. Oppenheim, A. K. Buell, D. Y. Chirgadze, M. E. Welland, *Nat. Nanotechnol.* **2010**, *5*, 204–207.

[3] J. W. Kelly, *Nat. Struct. Biol.* **2002**, *9*, 323–325.

[4] a) O. Inganas, P. Bjork, A. Herland, M. Hamedi, *J. Mater. Chem.* **2010**, *20*, 2269–2276; b) C. E. MacPhee, K. J. Channon, G. L. Devlin, S. W. Magennis, C. E. Finlayson, A. K. Tickler, C. Silva, *J. Am. Chem. Soc.* **2008**, *130*, 5487–5491; c) D. N. Woolfson, Z. N. Mahmoud, *Chem. Soc. Rev.* **2010**, *39*, 3464–3479.

[5] R. G. Ellis-Behnke, Y. X. Liang, S. W. You, D. K. C. Tay, S. G. Zhang, K. F. So, G. E. Schneider, *Proc. Natl. Acad. Sci. USA* **2006**, *103*, 7530–7530.

[6] S. L. Gras, A. K. Tickler, A. M. Squires, G. L. Devlin, M. A. Horton, C. M. Dobson, C. E. MacPhee, *Biomaterials* **2008**, *29*, 1553–1562.

[7] a) O. Inganas, H. Tanaka, A. Herland, L. J. Lindgren, T. Tsutsui, M. R. Andersson, *Nano Lett.* **2008**, *8*, 2858–2861; b) O. Inganas, A. Rizzo, N. Solin, L. J. Lindgren, M. R. Andersson, *Nano Lett.* **2010**, *10*, 2225–2230.

[8] a) L. Sawyer, G. Kontopidis, C. Holt, *J. Dairy Sci.* **2004**, *87*, 785–796; b) H. M. Ma, S. Y. Dong, Z. W. Zhao, *J. Proteome Res.* **2006**, *5*, 26–31; c) L. Sawyer, S. Brownlow, I. Polikarpov, S. Y. Wu, *Int. Dairy J.* **1998**, *8*, 65–72; d) L. Sawyer, G. Kontopidis, *BBA-Protein Struct M* **2000**, *1482*, 136–148.

[9] a) D. R. Flower, *Biochem. J.* **1996**, *318*, 1–14; b) K. Strzalka, J. Grzyb, D. Latowski, *J. Plant Physiol.* **2006**, *163*, 895–915.

[10] a) B. Akerstrom, D. R. Flower, J. P. Salier, *Biochim. Biophys. Acta - Protein Struct. Mol. Enzymol.* **2000**, *1482*, 1–8; b) A. Skerra, D. A. Breustedt, D. L. Schonfeld, *BBA-Proteins Proteom.* **2006**, *1764*, 161–173.

[11] F. Zsila, E. Hazai, L. Sawyer, *J. Agr. Food Chem.* **2005**, *53*, 10179–10185.

[12] C. J. Chen, M. C. Yang, H. H. Guan, M. Y. Liu, Y. H. Lin, J. M. Yang, W. L. Chen, S. J. T. Mao, *Proteins* **2008**, *71*, 1197–1210.

[13] M. Narayan, L. J. Berliner, *Biochem.-Us* **1997**, *36*, 1906–1911.

[14] C. Yu, S. Srisailam, H. M. Wang, T. K. S. Kumar, D. Rajalingam, V. Sivaraja, H. S. Sheu, Y. C. Chang, *J Biol Chem* **2002**, *277*, 19027–19036.

[15] a) L. Sawyer, G. Kontopidis, C. Holt, *J. Mol. Biol.* **2002**, *318*, 1043–1055; b) P. Mariani, G. Baldini, S. Beretta, G. Chirico, H. Franz, E. Maccioni, F. Spinozzi, *Macromolecules* **1999**, *32*, 6128–6138.

[16] a) M. R. Juchau, H. Chen, W. N. Howald, *Drug Metab. Dispos.* **2000**, *28*, 315–322; b) B. A. Conley, M. J. Egorin, R. Sridhara, R. Finley, R. Hemady, S. L. Wu, N. S. Tait, D. A. VanEcho, *Cancer Chemother. Pharm.* **1997**, *39*, 291–299; c) K. Palczewski, A. R. Moise, V. Kuksa, W. S. Blaner, W. Baehr, *J. Biol. Chem.* **2005**, *280*, 27815–27825.

[17] Y. J. Cho, C. A. Batt, L. Sawyer, *J. Biol. Chem.* **1994**, *269*, 11102–11107.

[18] L. M. Scolaro, M. Castriciano, A. Romeo, S. Patane, E. Cefali, M. Allegrini, *J. Phys. Chem. B* **2002**, *106*, 2453–2459.

© 2012 WILEY-VCH Verlag GmbH & Co. KGaA, Weinheim

[19] a) E. Dufour, M. C. Marden, T. Haertle, *FEBS Lett.* **1990**, *277*, 223–226; b) L. Brancaleon, F. Tian, K. Johnson, A. E. Lesar, H. Moseley, J. Ferguson, I. D. W. Samuel, A. Mazzini, *Biochim. Biophys. Acta - Gen. Subjects* **2006**, *1760*, 38–46.
[20] I. Inamura, K. Uchida, *Bull. Chem. Soc. Jpn.* **1991**, *64*, 2005–2007.
[21] L. Brancaleon, S. W. Magennis, I. D. W. Samuel, E. Namdas, A. Lesar, H. Moseley, *Biophys Chem* **2004**, *109*, 351–360.
[22] a) H. J. Wolfson, D. Schneidman-Duhovny, Y. Inbar, V. Polak, M. Shatsky, I. Halperin, H. Benyamini, A. Barzilai, O. Dror, N. Haspel, R. Nussinov, *Proteins-Struct. Funct. Genet.* **2003**, *52*, 107–112; b) H. Benyamini, A. Shulman-Peleg, H. J. Wolfson, B. Belgorodsky, L. Fadeev, M. Gozin, *Bioconjugate Chem* **2006**, *17*, 378–386.
[23] G. B. Jameson, B. Y. Qin, M. C. Bewley, L. K. Creamer, H. M. Baker, E. N. Baker, *Biochem.-Us* **1998**, *37*, 14014–14023.
[24] H. Molinari, L. Ragona, F. Fogolari, M. Catalano, R. Ugolini, L. Zetta, *J. Biol. Chem.* **2003**, *278*, 38840–38846.
[25] W. N. Lanzilotta, A. Medlock, L. Swartz, T. A. Dailey, H. A. Dailey, *Proc. Natl. Acad. Sci .USA* **2007**, *104*, 1789–1793.
[26] M. Gozin, B. Belgorodsky, L. Fadeev, J. Kolsenik, *Bioconjugate Chem.* **2007**, *18*, 1095–1100.
[27] H. Sun, R. Kawaguchi, J. M. Yu, J. Honda, J. Hu, J. Whitelegge, P. P. Ping, P. Wiita, D. Bok, *Science* **2007**, *315*, 820–825.
[28] a) D. S. Talaga, X. L. He, J. T. Giurleo, *J. Mol. Biol.* **2010**, *395*, 134–154; b) T. V. Burova, N. V. Grinberg, R. W. Visschers, V. Y. Grinberg, C. G. de Kruif, *Eur. J. Biochem.* **2002**, *269*, 3958–3968.
[29] a) C. Akkermans, P. Venema, A. J. van der Goot, H. Gruppen, E. J. Bakx, R. M. Boom, E. van der Linden, *Biomacromolecules* **2008**, *9*, 1474–1479; b) E. Dufour, C. Genot, T. Haertle, *BBA-Protein Struct. M* **1994**, *1205*, 105–112; c) S. Iametti, A. Barbiroli, F. Bonomi, P. Ferranti, D. Fessas, A. Nasi, P. Rasmussen, *J. Agr. Food Chem.* **2011**, *59*, 5729–5737; d) M. A. M. Hoffmann, G. Sala, C. Olieman, K. G. de Kruif, *J. Agr. Food Chem.* **1997**, *45*, 2949–2957; e) Y. D. Livney, *Cur. Opin. Colloid Interface Sci.* **2010**, *15*, 73–83; f) R. Piazza, *Curr. Opin. Colloid Interface Sci.* **2004**, *8*, 515–522; g) M. A. M. Hoffmann, J. C. van Miltenburg, J. P. van der Eerden, P. J. J. M. van Mil, C. G. de Kruif, *J. Phys. Chem. B* **1997**, *101*, 6988–6994.
[30] K. P. Das, C. Bhattacharjee, S. Saha, A. Biswas, M. Kundu, L. Ghosh, *Protein J.* **2005**, *24*, 27–35.
[31] a) A. Herland, D. Thomsson, O. Mirzov, I. G. Scheblykin, O. Inganas, *J. Mater. Chem.* **2008**, *18*, 126–132; b) A. Herland, P. Bjork, K. P. R. Nilsson, J. D. M. Olsson, P. Asberg, P. Konradsson, P. Hammarstrom, O. Inganas, *Adv. Mater.* **2005**, *17*, 1703–1703.
[32] a) R. F. Pasternack, C. Bustamante, P. J. Collings, A. Giannetto, E. J. Gibbs, *J. Am. Chem. Soc.* **1993**, *115*, 5393–5399; b) R. F. Pasternack, P. J. Collings, *Science* **1995**, *269*, 935–939.
[33] a) M. Gozin, B. Belgorodsky, L. Fadeev, V. Ittah, H. Benyamini, S. Zelner, D. Huppert, A. B. Kotlyar, *Bioconjugate Chem* **2005**, *16*, 1058–1062; b) L. L. Dugan, D. M. Turetsky, C. Du, D. Lobner, M. Wheeler, C. R. Almli, C. K. F. Shen, T. Y. Luh, D. W. Choi, T. S. Lin, *Proc. Natl. Acad. Sci. USA* **1997**, *94*, 9434–9439; c) C. Larroque, S. Foley, A. D. M. Curtis, A. Hirsch, M. Brettreich, A. Pelegrin, P. Seta, *Fullerene, Nanotubes Carbon Nanostruct.* **2002**, *10*, 49–67.
[34] W. W. de Jong, P. J. L. Werten, B. Roll, D. M. F. van Aalten, *Proc. Natl. Acad. Sci. USA* **2000**, *97*, 3282–3287.
[35] S. Brownlow, J. H. M. Cabral, R. Cooper, D. R. Flower, S. J. Yewdall, I. Polikarpov, A. C. T. North, L. Sawyer, *Structure* **1997**, *5*, 481–495.
[36] T. E. Ferrin, E. F. Pettersen, T. D. Goddard, C. C. Huang, G. S. Couch, D. M. Greenblatt, E. C. Meng, *J. Comput .Chem.* **2004**, *25*, 1605–1612.

© 2012 WILEY-VCH Verlag GmbH & Co. KGaA, Weinheim